

# Finite Element Analysis of Sheet Metal Air-bending Using Hyperform LS-DYNA

Himanshu V. Gajjar, Anish H. Gandhi, and Harit K. Raval

**Abstract**—Air bending is one of the important metal forming processes, because of its simplicity and large field application. Accuracy of analytical and empirical models reported for the analysis of bending processes is governed by simplifying assumption and do not consider the effect of dynamic parameters. Number of researches is reported on the finite element analysis (FEA) of V-bending, U-bending, and air V-bending processes. FEA of bending is found to be very sensitive to many physical and numerical parameters. FE models must be computationally efficient for practical use. Reported work shows the 3D FEA of air bending process using Hyperform LS-DYNA and its comparison with, published 3D FEA results of air bending in Ansys LS-DYNA and experimental results. Observing the planer symmetry and based on the assumption of plane strain condition, air bending problem was modeled in 2D with symmetric boundary condition in width. Stress-strain results of 2D FEA were compared with 3D FEA results and experiments. Simplification of air bending problem from 3D to 2D resulted into tremendous reduction in the solution time with only marginal effect on stress-strain results. FE model simplification by studying the problem symmetry is more efficient and practical approach for solution of more complex large dimensions slow forming processes.

**Keywords**—Air V-bending, Finite element analysis, Hyperform LS-DYNA, Planner symmetry.

## I. INTRODUCTION

**M**OST sheet metal-forming processes involve bending of initial blank. Air bending is the simplest bending process commonly used in automotive stamping and fabrication industries. It has advantage over other bending processes, since there is no need to change the dies to obtain different bending angles. Fig. 1 shows the schematics of air V-bending process. For the set die opening ( $W_d$ ), punch travel ( $d$ ) controls the bend angle ( $\theta$ ). Accurate bend allowance and

springback predictions are important to maintain the geometric tolerance of the finished part. Springback refers to the elastic recovery of the non-uniformly distributed stresses in a deformed part after the forming load is removed. Bend allowance is a parameter that compensate for the elongation of sheet in bending.

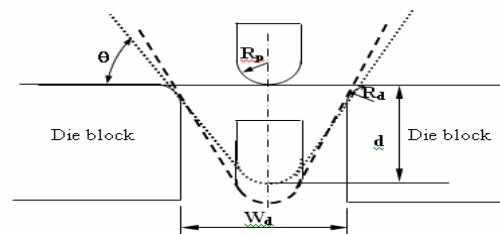


Fig. 1 Schematics of air V-bending process

Literature survey shows that considerable amount of researches are reported on modeling (including analytical, empirical and FE) and analysis of V-bending, U-bending, air V-bending etc. Few important literatures are briefly discussed here.

Martin and Tsang [1] presented a theoretical and experimental analysis of the behavior of simply supported beam bent by central load while freely supported at the ends considering plane strain, plane stress conditions and the effect of friction at contact interfaces. Wang et al. [2] reported mathematical models for plain-strain sheet bending to predict; spring back, bendability, strain and stress distributions and the maximum loads on the punch and the die. Vin et al. [3] reported, 'three section' model for air V-bending. The material behavior was described by the Swift's equation and the change of Young's modulus under deformation was addressed. Leu [4] reported that precise prediction of the springback and bendability are the key factor for the design of the bending tool, controlling the bending process and assessing the accuracy of part geometry. Date et al. [5] reported the process model to assess the effect of different geometric and material parameters on the springback in the air V-bending process. Gau and Kinzel [6] investigated the influence of Bauschinger effect on springback in sheet metal forming. Inamdar et al. [7] performed the experiments to study the effect of geometric parameters on springback in sheets of five different materials for air V-bending. Raval [8] reported the simulation program for the prediction of punch travel to bend the plate at desired angle, gap formation under the punch

Manuscript received September 05, 2007. This work is the part of Master of Technology thesis submitted to Sardar Vallabhbhai National Institute of Technology (Deemed University), Surat-395007, Gujarat, India during the academic year of 2006-07.

Himanshu V. Gajjar is a student of Master of Technology in Mechanical Engineering Department (MED) at Sardar Vallabhbhai National Institute of Technology (Deemed University), Surat-395007, Gujarat, India (e-mail: hvgajjar@hotmail.com).

Anish H. Gandhi, is a Ph. D. Research Scholar in Mechanical Engineering Department at Sardar Vallabhbhai National Institute of Technology (Deemed University), Surat-395007, Gujarat, India (Corresponding Author; e-mail: anishgandhi2002@yahoo.co.in, ahg@med.svnit.ac.in, phone: +91 261 2766265, (M) +91 9374519605).

Harit K. Raval is a Professor, Mechanical Engineering Department, Sardar Vallabhbhai National Institute of Technology (Deemed University), Surat-395007, Gujarat, India (e-mail: hkr@med.svnit.ac.in).

and springback in air V-bending process. Gandhi et al. [9], [10] simulated the multiple pass air V-bending using change of modulus of elasticity during bending.

Li et al. [11] performed FE springback simulations of V-free bending, using a self developed 2D elasto-plastic finite element program. Material model considered were linear hardening and elsto-plastic power-exponent with the change of Young's modulus during the deformation. Satorres [12] attempted the FE analysis of air bending in Ansys LS-DYNA and reported that 10 times to 100 times mass scaling can be used to reduce solution time without major effect on results. He also reported that the velocity scaling can be used for further reduction in solution time but real velocity should be used to get accurate results. Dutton [13] performed FE simulation of sheet metal forming and suggested that LS-DYNA solver is the best tool for springback analysis. Gantner and Bauer [14] worked with the FE simulation of complex bending processes by using the nonlinear simulation program LS-DYNA and suggested that it is the best solver for the crash analysis and simulation. Verma and Haldar [15] reported the effect of anisotropy on springback using FEA for the benchmark problem of Numisheet-2005. Analytical model was developed to crosscheck the trend predicted by the FEA. They concluded that higher the anisotropy, higher the springback and FEA result shows the minimum springback for isotropic material.

Accuracy of analytical and empirical models reported for the analysis of bending processes is governed by simplifying assumption and do not consider the effect of dynamic parameters. Finite element simulation was performed by number of researchers to study the effect of various machine parameters (i.e. die radius, punch radius, die gap and blank holding force), geometry parameters (i.e. plate thickness and bend angle), material models (i.e. isotropic hardening, kinematic hardening etc.) and FE modeling parameters (i.e. element type, contact damping parameter, penalty parameter, element size, numerical corner element, punch velocity). Along with the accuracy, solution time for FEA is an important parameter. Solution time depends on number of factors such as computational facility available, number of elements, size of elements, time step size, punch velocity, number of integration point, minimum edge length of element etc. Finite element models must be computationally efficient for practical use.

Presented work shows the 3D FE modeling of air V-bending in Hyperform. Problem was solved in non linear dynamic solver LS-DYNA. Results of 3D FEA with Hyperform LS-DYNA were compared with published 3D FEA results with Ansys LS-DYNA [12]. FEA bending stress and strain results were also verified with the published experimental stress strain results obtained from tensile testing of specimens cut at  $0^\circ$  and  $90^\circ$  to rolling direction and were found to be in good agreement [12]. Further looking to the planer symmetry of air V bending process, modeling was simplified from 3D to 2D assuming plane strain condition (width to thickness ratio greater than 8) [16]. Stress-strain

results and solution time of 3D FEA were compared with that obtained from simplified 2D FEA. It was observed that simplification of the problem from 3D to 2D after studying the problem symmetry, resulted into the large reduction in the number of elements and hence simplified 2D FE models can be solve without any velocity and/or mass scaling with acceptable accuracy. Reported concept can be applied for the FEA of more complex and larger dimensions slow forming problems like roller bending, extrusion, forging etc.

## II. 3-D FINITE ELEMENT MODELING

Fig. 2 shows the general work flow diagram adapted to model and solves the air V-bending problem by FEA. The punch and die set assembly along with the specimen was modeled in CATIA v5 and exported as \*.IGS in Hyperform.

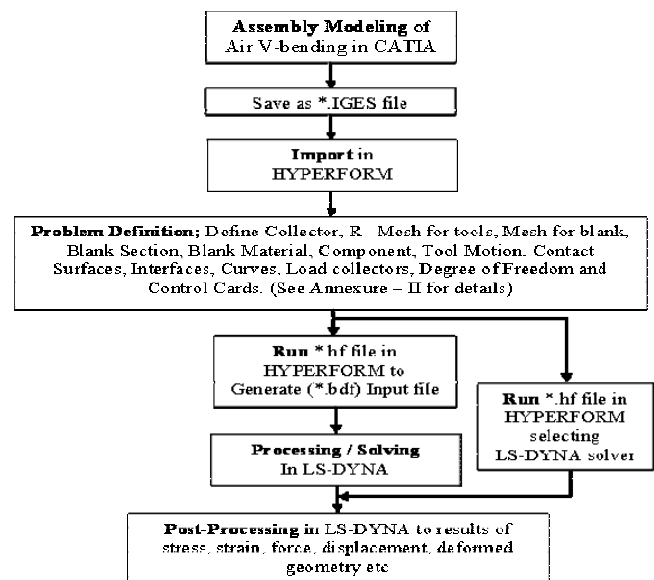


Fig. 2 General Block Diagram of work flow

FE model of air V-bending process was defined in Hyperform v7.0 and solved in LS-DYNA970. Geometrical set-up, process parameters, material models and FE parameters used for the presented analysis are discussed in foregoing sections.

### A. Model Geometry

Fig. 3 shows the geometrical model used for the FE analysis. For the presented cases, 300 mm x 300 mm (length x width) raw material blank with two different thicknesses of 3 mm and 6 mm were selected. Two different die gaps (G) of 50 mm and 76 mm were selected for 3 mm and 6 mm thick blanks respectively. For 3 mm and 6 mm thick blanks, die radius ( $R_d$ ) selected was 5 mm and 7 mm respectively. Punch radius of 5 mm was selected for all the cases. All the geometrical parameters were kept same as reported in literature [12] for comparison of results.

### B. Meshing

Each part of the air V-bending assembly (i.e. punch, dies, blank) was meshed separately in Hyperform 7.0. Blank was mapped mesh with eight noded brick elements (Solid elements). Table I shows the mesh parameters used for FE modeling of different parts. The blank of 3 mm and 6 mm were meshed with 90 elements (with approximate element size of 3.3 mm x 3.3 mm) in width and length. Whereas, two elements were kept in thickness direction so, element size is 1.5 mm and 3 mm for blank having 3 mm and 6 mm thickness respectively. The die and punch were meshed with 20 number of element on all four edges for both the blank thickness. Punch and die set was defined as a rigid body.

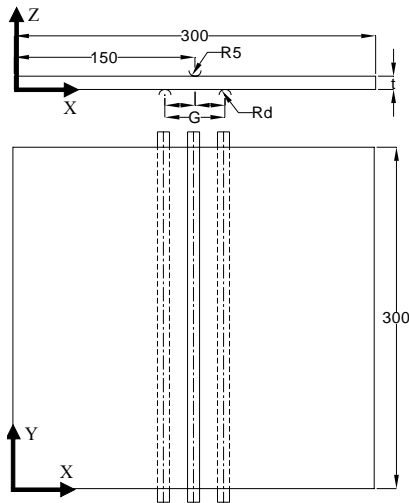


Fig. 3 Model Geometry

TABLE I

MESH PARAMETERS [12]

Part	Introduced mesh	No. of nodes	No. of elements	Approximate element size (mm)
Blank (3 mm)	2-90-90	24,843	16,200	1.5*3.3*3.3
Blank (6 mm)	2-90-90	24,843	16,200	3*3.3*3.3
Punch	20-20-20-20	441	400	17*0.78
Die	20-20-20-20	441	400	17*0.94

### C. Material Property

Tensile testing of HSLA steel specimens prepared at  $0^\circ$ ,  $45^\circ$  and  $90^\circ$  to the rolling direction was performed by Satorres [12]. Reported experimental stress-strain curves for 3 mm and 6 mm thick HSLA steel sheets as shown in Fig. 4 and 5 were used as an input for selected material model 24 (MAT\_PIECEWISE\_LINEAR\_PLASTICITY) [17].

### D. Tool Motion

Displacement loading condition was applied with the total punch travel of 13.5 mm at velocity of 19 mm/sec. Actual punch velocity during experimentation was 9.5 mm/sec. For reduction in the solution time for FEA, velocity scaling of 2 was used.

### E. Contact Definition

Contact interface between punch and blank and die and blank were defined by contact option FORMING\_ONE\_WAY\_SURFACE\_TO\_SURFACE [17] with friction coefficient of 0.4 between punch and blank and 0.2 between die and blank [12]. Punch and die set was constrained in rotations about all three principal axes. Die set translations in all three principal axes were constrained where as, punch was assign translation degree of freedom in z axis direction (i.e. in the direction of punch movement) to apply the load.

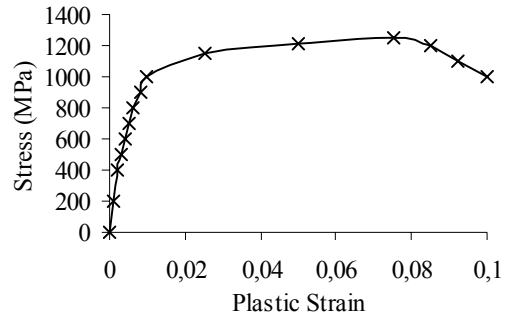


Fig. 4 Stress strain curve for 3 mm thick blank at  $0^\circ$  direction

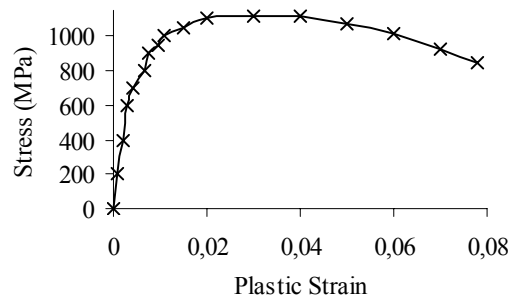


Fig. 5 Stress strain curve for 6 mm thick blank at  $0^\circ$  direction

### F. Density Mass Scaling

For further reduction in the solution time for FEA, density of punch, die and blank material was scaled by factor 100 (i.e. density value of  $7.815E-07$  tones/ $\text{mm}^3$  instead of  $7.815E-09$  tones/ $\text{mm}^3$ ) [12].

### G. Control Cards

Control cards activation is required to set the solver specific data. Different control cards such as; keywords, hourglass, control shell, control termination, control contacts, control time steps, database binary extent, database d3plot, database options, etc. were used for presented analysis along with the various parameter values as reported in appendix. Control cards selection depends on mechanics of the problem, FE modeling and outputs required [17].

## III. 2-D FINITE ELEMENT MODELING

Based on observed planner symmetry (in XZ plane or Y plane) in case of air V-bending (refer Fig. 3) and assumption

of plane strain condition (width to the thickness ratio greater than 8), air V-bending process was modeled in two dimensions (2D) with symmetric boundary conditions along the width of the plate. Mapped mesh with four noded quadrilateral shell element (QUAD4) was used for FE modeling of blank. TYPE16: fully integrated shell element [17] was selected for the presented analysis. Punch and die set was defined as a rigid body. Material model, tool motion, contact definitions were kept same as that of the 3D FE model discussed in section II. Table II shows the comparison of mesh parameters for 2D and 3D FE modeling. Total number of node reduces to 1,107 in case of 2D from that of total 25,725 numbers of nodes in case of 3D FE modeling.

TABLE II  
COMPARISON OF MESH PARAMETERS

Part	3D FEM (Solid Element)			2D FEM (Shell Element, QUAD4, 0.1 mm thick)		
	Introduced mesh	No. of nodes	No. of elements	Introduced mesh	No. of nodes	No. of elements
Blank	2-90-90	24,843	16,200	2, 90, 90	273	180
Punch	20-20-20-20	441	400	20, 20	417	303
Die	20-20-20-20	441	400	20, 20	417	303
Total	-	25,725	17,000	-	1,107	786

IV. RESULTS AND DISCUSSION

The stress-strain results obtained from 3D FEA of air V-bending in Hyperform LS-DYNA were compared with the FEA results based on Ansys LS-Dyna and experimental results reported in literature [12].

Fig. 6 shows the maximum bending stress generated during the bending at the time interval of 0.468 sec for the presented analysis along with the generated bending stress fringes for 3 mm thick blank. Fig. 7 shows the plastic strain generated at 0.755 sec for 3 mm thick blank cut along the rolling direction. Table III shows the comparison of 3D FEA results of maximum bending stress and maximum plastic strain for 3 mm thick blank with the results reported in literature [12]. Fig. 8 shows the comparison of stress-strain curve obtained from 3D FEA in Hyperform LS-DYNA with published 3D FEA results based on Ansys LS-DYNA and experimental stress-strain readings of tensile testing with blank cut along rolling direction. Figs. 9 and 10 shows the maximum bending stress along with the stress fringes and maximum plastic strain obtains from 3D FEA in Hyperform LS-DYNA for 6 mm thick blank cut along the rolling direction. Stress-strain results comparisons for 6 mm thick blank cut along the rolling direction are reported in Fig. 11 and Table IV. Close agreement of 3D FEA results of air V-bending from Hyperform LS-DYNA with the reported FEA and experimental results proves the correctness of the FE modeling procedure.

On comparison of FEA stress vs. plastic strain results of 3 mm and 6 mm thick blank with the published FEA and experimental results (refer Fig. 8 and 11) it was observed that FEA stress results were found to be higher than that of the experimental stress results. This may be due to higher

assumed value of coefficient of friction (i.e. 0.2) at die work piece interface and punch velocity scaling for the reduction in the solution time. Bending load is very sensitive to coefficient of friction at tool work piece interfaces. Friction coefficient at die work piece interface should be of sliding friction range. Higher punch velocity will results into the higher bending force due to kinematics effect.

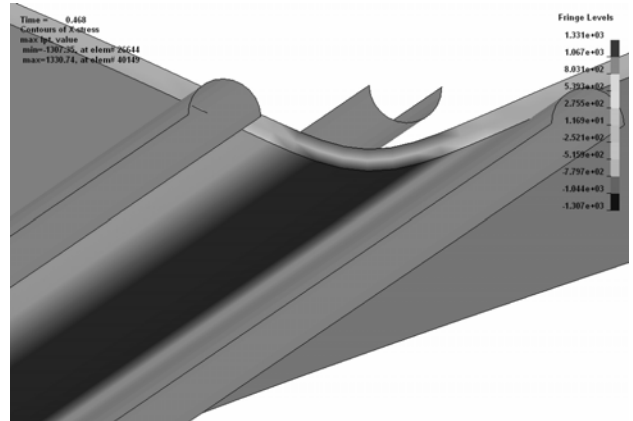


Fig. 6 Stress values in 3 mm thick blank at t=0.468 sec, d=8.89 mm

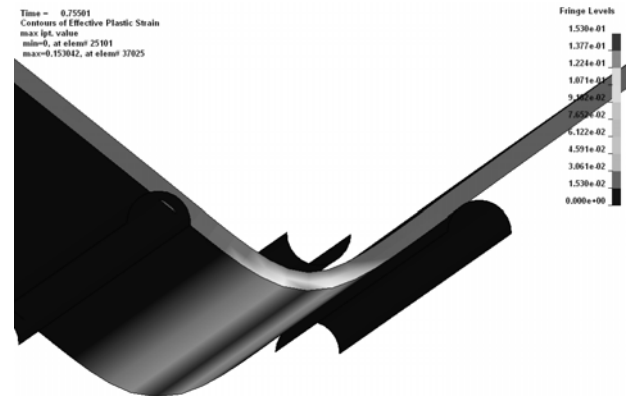


Fig. 7 Plastic strain in 3 mm thick blank at t=0.75501 sec

TABLE III  
COMPARISON OF FEA RESULTS WITH PUBLISHED LITERATURE, 3 MM THICK BLANK

Stress (MPa)			Plastic strain		
Published FEA Results [12]	FEA results Hyperform LS-Dyna	% Error	Published FEA Results [12]	FEA results Hyperform LS-Dyna	% Error
1353.7	1330.7	1.69	0.145	0.153	-5.51

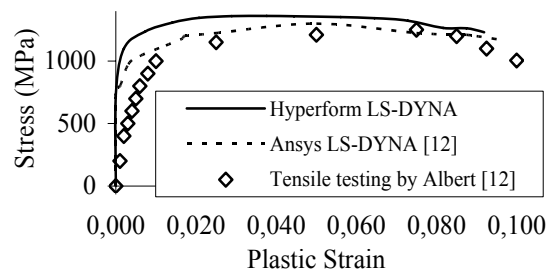


Fig. 8 Stress strain curve comparison for 3 mm thick blank

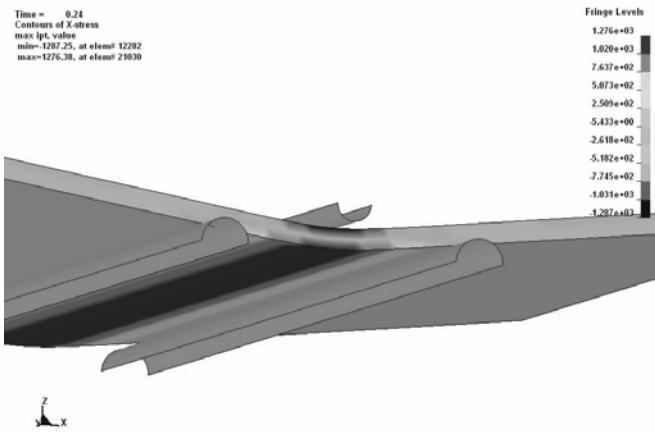


Fig. 9 Stress values in 6 mm thick blank at t=0.24 s

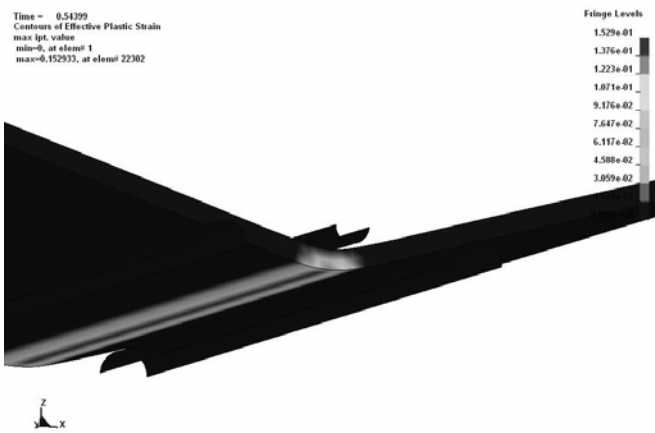


Fig. 10 Plastic strain for 6 mm thick blank at t=0.54399 s

TABLE IV  
COMPARISON OF FEA RESULTS WITH PUBLISHED LITERATURE, 6 MM THICK BLANK

Stress (MPa)			Plastic strain		
Published FEA Results [12]	FEA results Hyperform LS-Dyna	% Error	Published FEA Results [12]	FEA results Hyperform LS-Dyna	% Error
1282	1276	0.4	0.151	0.153	-1.25

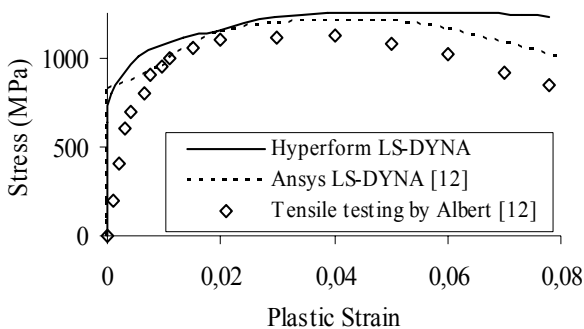


Fig. 11 Stress strain curve comparison for 6 mm thick blank

From Fig. 6 and 7 for 3 mm thick blank and Fig. 9 and 10 for 6 mm thick blank for FE bending stress and plastic strain

results, it can be observed that stress and strain fringe pattern in the width (i.e. Y axis) direction is uniform. So, air V-bending problem is having planner symmetry in Y plane (or XZ plane). For the selected blanks, width to thickness ratio is greater than 8. So, 3D FE model of air V-bending can be simplified to the 2D FE model with symmetric boundary condition in width. Table V shows the comparison of bending stress and plastic strain results of 3D and 2D FEA with published results along with the solution time. Due to reduction in number of nodes from 3D to 2D FEA (refer Table II), solution time for 2D FEA reduced to 5 minutes from that of 56 minutes in case of 3D FEA with marginal effect on stress and strain results.

Though same solver was used for the FEA along with the similar boundary conditions as reported in literature [12], deviation was observed in the results obtained from FEA in Hyperform LS-DYNA from that of published results. Variation observed may be due to the following reasons;

1. The stress-strain result obtained from FEA in Hyperform LS-DYNA depends on values of input material property parameters. In the present analysis the value of strength coefficient (K) and strain hardening exponent (n) was obtained from the plotted stress strain curve, which might be different than values used in published literature [12].
2. Model geometry distortion while importing the \*.IGES file into the FE modeling software.

TABLE V  
COMPARISON OF 2D AND 3D FEA RESULTS

t (mm)	FEA results [12]	FEA results on Hyperform LS-DYNA					
		3D FEA			2D FEA		
		Stress <sup>1</sup> / Strain	% Error	Time <sup>2</sup>	Stress <sup>1</sup> / Strain	% Error	Time <sup>2</sup>
3	1353	1330.7	1.69	56	1196	12.9	5
	0.145	0.153	-5.51		0.155	-6.4	
6	1282	1276.3	0.4	56	1176	8.26	5
	0.151	0.1529	-1.25		0.156	-3.31	

<sup>1</sup>Bending stress results in MPa, <sup>2</sup>Actual solution time in minutes

## V. CONCLUSION

Results obtained from the FEA analysis performed in the Hyperform LS-DYNA is found to be in good agreement with the published FEM results from Ansys LS-DYNA and experimental stress strain results. Following important conclusion can be made out of the reported analysis;

1. LS-DYNA is a good tool to simulate sheet metal bending processes.
2. FEA can be helpful to study the effect of kinematics parameters like punch speed and coefficient of friction at tool-blank interfaces on resulting stress-strains mechanisms and hence formability.
3. Accuracy of the FEA results and solution time depends on the FE modeling parameter selection.
4. Instead of using mass scaling and velocity scaling as an option for reduction in solution time, FE model simplification by studying the problem symmetry is more efficient and practical approach for solution of more

complex large dimensions slow forming processes.

APPENDIX

```
*KEYWORD
SS HM_OUTPUT_DECK created 12:36:40 03-10-2007 by HyperMesh Version 7.0
SS Ls-dyna Input Deck Generated by HyperMesh Version : 7.0
SS Generated using HyperMesh-Ls-dyna 970 Template Version : 7.0
*CONTROL_TERMINATION
SS ENDTIM ENDCYC DTMIN ENDENG ENDMAS
0.755
*CONTROL_TIMESTEP
SS DTINIT TSSFAC ISDO TSLIMIT DT2MS LCTM ERODE MSIST
0.9 1.1000E-05
*CONTROL_SHELL
SS WRPANG ESORT IRNXX ISTUPD THEORY BWC MITER PROJ
20.0 0 -1 0 2 2
*CONTROL_HOURLASS
SS IHQ QH
4
*CONTROL_CONTACT
SS SLSFAC RWPNAL ISLCHK SHLTHK PENOPT THKCHG ORIEN ENMSS
0.1 0.0 0 1 0 1 0
SS USRSTR USRFRC NSBCS INTERM XPENE SSTHK ECDT TIEDPRJ
*CONTROL_OUTPUT
SS NPOPT NEECHO NREFUP IACCOP OPIFS IPNINT IKEDIT
0 0 0 0 0.0
*CONTROL_ENERGY
SS HGEN RWEN SLNTEN RYLEN
1 1 2 1
SSDATABASE_OPTION -- Control Cards for ASCII output
*DATABASE_BNDOUT
1.0000E-03 1
*DATABASE_ELOUT
1.0000E-03 1
*DATABASE_GCEOUT
1.0000E-03 1
*DATABASE_GLSTAT
1.0000E-03 1
*DATABASE_MATSUM
1.0000E-03 1
*DATABASE_RCFORC
1.0000E-03 1
*DATABASE_BINARY_D3PLOT
SS DT/CYCL LCDT BEAM NPLTC
0.004
0
*DATABASE_BINARY_D3THDT
SS DT/CYCL LCD
0.002
*DATABASE_BINARY_D3DUMP
SS DT/CYCL
0.02
*DATABASE_EXTENT_AVS
SS VTYPE COMP
4 3
*DATABASE_EXTENT_BINARY
SS NEIPH NEIPS MAXINT STRFLG SIGFLG EPSFLG RLFLG ENGLFG
0 0 3 1 1 1 1 1
SS CMPFLG IEVERP BEAMIP DCOMP SHGE STSS N3THDT
0 0 0
SS NINTSLD
*INCLUDE
nodes.k
*MAT_RIGID
SHMNAME MATS 5Punch_mat
57.8150E-07 202465.0 0.28
1.0 4 7
*MAT_RIGID
SHMNAME MATS 6die_mat
67.8150E-07 202465.0 0.28
1.0 7 7
*MAT_PIECEWISE_LINEAR_PLASTICITY
SHMNAME MATS 3PI_mat
37.8150E-07 202465.0 0.28 851.7 0.0 0.0 0.0
0.0 0.0 1.0 0 0
SS HM Entries in Stress-Strain Curve = 0
*PART
SHMNAME COMPS 1blank
SHMCOLOR COMPS 1 9
1 1 3 0 0 0 0
SHMNAME COMPS 2Punch
SHMCOLOR COMPS 2 7
2 2 5 0 0 0 0
SHMNAME COMPS 3die
SHMCOLOR COMPS 3 15
3 2 6 0 0 0 0
*SECTION_SHELL
SHMNAME PROPS 2tool_sec
2 2 0.0 0.0 0
0.1 0.1 0.1 0.1 0.0
*SECTION_SOLID
SHMNAME PROPS 1Bl_sec
1
*BOUNDARY_PRESCRIBED_MOTION_RIGID
SHMNAME LOADCOLS 1Loadcol_PrerbRgB-Punch
SHMCOLOR LOADCOLS 1 12
2 3 2 1.0 0
*INCLUDE
set_segment_punch.k
*INCLUDE
set_segment_die.k
*CONTACT_ONE_WAY_SURFACE_TO_SURFACE_ID
SHMNAME GROUPS 1PC2BC
SHMCOLOR GROUPS 1 1
1
3 1 0 0
0.4 3 1 0 0 20.0 5.0
*CONTACT_ONE_WAY_SURFACE_TO_SURFACE_ID
SHMNAME GROUPS 2DC2BC
```

```
SHMCOLOR GROUPS 2 1
2
3 2 0 0
0.2 20.0 5.0
*INCLUDE
elements1.k
*INCLUDE
elements2.k
*INCLUDE
curve_3mm.k
*DEFINE_CURVE
SHMNAME CURVES 2PrerbRgB_curve-Punch
SHMCOLOR CURVES 2 12
SHMCURVE 1 1
2 0 1.0 1.0 0.0 0.0 0
0.0 0.0
0.04 -19.0
0.75 -19.0
0.751 0.0
*END
SHMASSEM 1 1101:SubfigureDefinition
SHMASSEM_COMP_IDS 1
SHMASSEM 2 1173:SubfigureDefinition
SHMASSEM_COMP_IDS 2
SHMASSEM 3 1305:SubfigureDefinition
SHMASSEM_COMP_IDS 3
```

REFERENCES

- [1] G. Martin and S. Tsang, "The Plastic Bending of beams Considering Die Friction Effects," Transaction of ASME, J. Eng. Ind., pp. 237-250, August 1966.
- [2] Chuan to Wang, Gary Kinzel and Taylan Altan, "Mathematical modeling of plane-strain bending of sheets and plates," J. Mater. Process. Technol., vol. 39, pp 279-304, 1993.
- [3] L. J. de Vin, A. H. Streppel, U. P. Singh and H. J. J. Kals, "A process model for air bending," J. Mater. Process. Technol., vol. 57, pp. 48-54, 1996.
- [4] Daw-Kwei Leu, "A simplified Approach for Evaluating Bendability and Springback in Plastic Bending of Anisotropic Sheet Metals," J. Mater. Process. Technol., vol. 66, pp. 9-17, 1997.
- [5] P. P. Date, K. Narasimhan, S. K. Maiti and U. P. Singh, "On the prediction of spring back in Vee- Bending of metallic sheets under plane strain condition," Sheet Metal, Sept 1999, pp 447-456.
- [6] Jenn-Terng Gau and Gary L. Kinzel, "An Experimental Investigation of the Influence of the Bauschinger Effect on Springback Predictions," J. Mater. Process. Technol., vol. 108, pp. 369-375, 2001.
- [7] M. V. Inamdar, P. P. Date, K. Narsimhan, S. K. Maiti and U. P. Singh, "Development of Artificial Neural Network to predict springback in air V bending," J. adv. Manuf. Technol., vol. 16, pp. 376-381, 2000.
- [8] H. K. Raval, "Experimental & Theoretical Investigation of Bending Process, (Vee & Three Roller bending)," PhD dissertation, South Gujarat University, India, 2002.
- [9] A. H. Gandhi, G. J. Solanki and H. K. Raval, "Investigation on Multiple Pass Bending-A Simulation Study," Proc. Int. Conf. on Recent Advances in Mechanical & Materials Engg., Kuala Lumpur, Malaysia, 30-31 May 2005, pp 971-976.
- [10] A. H. Gandhi, G. J. Solanki and H. K. Raval, "On the effect of various parameters on springback and energy in multiple pass (Air vee) bending: part 1," Proc. 3rd Int. conf. on manuf. Research (ICMR2005), Cranfield University, UK, 6-8 Sept 2005.
- [11] Xuechun Li, Yuying Yang, Yongzhi Wang, Jun Bao and Shunping Li, "Effect of Material Hardening Mode on the Springback Simulation Accuracy of V-free Bending," J. Mater. Process. Technol., vol. 123, pp. 209-211, 2002.
- [12] Albert Satorres, "Bending simulation of High strength steel by finite elements", Master's thesis, University of Oulu, 2005. Available: [http://www.oulu.fi/elme/ELME2/PDF/Diplomityot/Masters\\_Thesis\\_Albert\\_Satorres%20.pdf](http://www.oulu.fi/elme/ELME2/PDF/Diplomityot/Masters_Thesis_Albert_Satorres%20.pdf).
- [13] Trevor Dutton, "Review of Sheet Metal Forming Simulation Progress to Date, Future Developments," 8th Int. LS-DYNA Users Conf., 2006.
- [14] Peter Gantner and Herbert Bauer, "FEA Simulation of Bending Processes with LS-DYNA," 8th Int. LS-DYNA Users Conf., 2006.
- [15] Rahul K. Verma and A. Haldar, "Effect of Normal Anisotropy on Springback," J. Mater. Process. Technol., to be published. doi:10.1016/j.jmatprotec.2007.02.033.
- [16] Duncan J. L., "The Mechanics of Sheet Metal Forming," Edward Arnold Ltd., London, 1992.
- [17] LS-DYNA Keyword Users Manual, Version 970, Livermore Software Technology Corporation (LSTC), April 2003.